Fat Embolism Syndrome: Lung Computed Tomography Findings in 18 Patients

Marco Piolanti, MD,* Giorgia Dalpiaz, MD,† Mariano Scaglione, MD,‡§ Carlo Coniglio, MD,‖ Marco Miceli, MD,* Sara Violini, MD,¶ Rocco Trisolini, MD,# and Libero Barozzi, MD*

Objective: The purpose of this study was to evaluate the lung computed tomography (CT) findings in fat embolism (FE) syndrome.

Methods: We retrospectively evaluated 19 CT examinations of 18 patients with FE syndrome, diagnosed clinically using the Gurd and Wilson criteria.

Result: Fat embolism syndrome showed 3 patterns: negative examination, bilateral interstitial-alveolar involvement, and adult respiratory distress syndrome like. Frequent findings included consolidations (17 patients), mostly with gravity dependent distribution, and ground-glass opacities (17 patients), mostly with patchy distribution. Fifteen patients showed an overlapping random nodular pattern. Less common findings included lobular ground-glass opacities and lobular consolidations, smooth septal thickening, thickening of the bronchial wall, and areas of crazy paving. The extension of the consolidations correlates with the duration of assisted ventilation.

Conclusions: In FE syndrome, pulmonary CT findings are ground-glass opacities and dependent consolidations, associated with other variably overlapping signs, such as lobular opacities, random nodules, septal thickening, and bronchial wall thickening.

Key Words: adult, embolism, fat, injuries, multidetector computed tomography, respiratory distress syndrome, spiral computed, thoracic, tomography

(*J Comput Assist Tomogr* 2016;00: 00–00)

The most frequent cause of fat embolism (FE) is bone fractures, especially those of the long bones, which occur in young patients. Pulmonary and systemic embolization is caused by the release of fat droplets into venous blood flow at the site of the fracture.[1] More rarely, posttraumatic FE may occur in the absence of fractures due to subcutaneous fat crushing.[2,3] There are also several nontraumatic causes of FE, which are not frequently encountered.[4] In most of the cases, FE occurs asymptomatically, without clinical consequences. However, in a minority of cases, the FE syndrome (FES) occurs, classically characterized by the combination of acute respiratory failure with central nervous system and cutaneous involvement. Clinical manifestations may occur after trauma (posttraumatic FES) or after surgical reduction of fractures (postoperative FES).[4]

In literature, the incidence of posttraumatic FES varies considerably, ranging from 0.25% up to 35%.[1] Fat embolism syndrome is diagnosed on the basis of the clinical features and by excluding other possible causes. As such, no investigation is 100% specific.[4] The diagnostic criteria that are most widely adopted are those from Gurd and Wilson[3] and those from Lindeque et al[5] (Table 1). The diagnosis is challenging in severely traumatized patients because of the overlapping of other body and cerebral lesions. In those cases, only the appearance of the petechial rash allows for the diagnosis of FES.[6]

The clinical presentation is classified into 3 different responses: classic response (characterized by transient pulmonary dysfunction), adult respiratory distress syndrome (ARDS), and hyperacute syndrome (with death within 48 hours).[7] The hyperacute syndrome, which is also called the fulminant form, is characterized by cardiovascular collapse and is the rarest presentation of all.

Radiological signs in conventional radiology are relatively nonspecific, demonstrate a lag time relative to the clinical symptoms, and are of little help in the differential diagnosis.[8–10] A few studies regarding the use of computed tomography (CT) are available in the literature.[11–14] There are also some case reports of macroscopic FE being detected with contrast-enhanced CT.[15–17] The purpose of our study was to assess the lung CT findings in a series of patients with a clinical diagnosis of FES, obtained using the diagnostic criteria of Gurd and Wilson.[3,5]

MATERIALS AND METHODS

This retrospective study was approved by the institutional review board of our institution (Comitato Etico, AUSL Bologna, Italy). Our series consist of 18 patients (14 males and 4 females) with clinical diagnosis of FES, based on the criteria of Gurd and Wilson[3] and a CT examination performed after the onset of respiratory failure.

To identify cases of FE that occurred at our institution between January 1, 2002, and December 31, 2014, we used the following strategies. The files of the radiology unit were searched for all the CT examinations performed with the following indications: (1) suspect FE and (2) respiratory failure in patients with trauma. These data were crossed with the diagnoses of FE found in the databases of the intensive care unit. In this way, we found 31 patients with clinical diagnosis of FES. After screening of the medical charts, 9 patients were excluded because the diagnosis did not fulfill the Gurd and Wilson[3] criteria, and 4 were excluded for the presence of severe thoracic trauma at admission. Diagnostic criteria for our 18 patients are displayed in Table 2.

The average age was 27 years (range, 18-58 years). Five patients were hospitalized in the intensive care unit, 5 patients were hospitalized in the orthopedic department, and 8 patients in both. Seven patients had posttraumatic FES, whereas in 11, FES followed the surgical fixation of the fractures.

Following the classification by Curtis et al,[7] the clinical presentations were categorized as transient pulmonary dysfunction, ARDS (following the criteria of the Berlin definition[18]), or as fulminant form, according to the degree of the respiratory failure.

Regarding the CT technique, because of the long period covered by this study, we found a heterogeneous sample. The examinations were performed on 5 different CT scanners and with

TABLE 1. Diagnostic Criteria of FES

Gurd and Wilson Criteria

Major criteria
  Petechial rash
  Respiratory insufficiency (hypoxemia)
  Cerebral involvement (confusion, stupor, coma)
Minor criteria
  Pyrexia
  Tachycardia
  Retinal changes
  Jaundice
  Renal signs
  Thrombocytopenia
  Anemia
  High erythrocyte sedimentation rate (ESR)
  Fat macroglobulinemia

Lindeque et al Criteria

Sustained PO_2 <60 mm Hg
Sustained PCO_2 >55 mm Hg or pH <7.3
Sustained respiratory rate >35 breaths/min, even after sedation
Increased work of breathing, dyspnea, tachycardia, and anxiety

Gurd and Wilson criteria require the presence of 2 major criteria or 1 major criterion with at least 4 minor criteria. The results of the arterial blood gas analysis are included in the criteria defined by Lindeque et al, where FES is diagnosed in presence of a femoral or a tibial fracture and of one of the criteria.

different acquisition protocols, although always with a volumetric acquisition. Two examinations were performed with a Tomoscan AV (Philips Healthcare, Best, the Netherlands) single slice spiral CT scanner, with slice thickness of 10 and 7 mm. Two were performed with a PQ 6000 (Picker International, Inc, Cleveland) single slice spiral CT scanner, with a slice thickness of 8 mm. Thirteen were performed with a 4-slice Hi-speed multislice (GE Healthcare, Little Chalfont, UK), with a slice thickness 5 of mm in 7, 2.5 mm in 3, and 1.25 in 3. One was performed with a 40-slice Somatom Sensation (Siemens Healthcare, Erlangen, DE), with a slice thickness of 2 mm. One was performed with a 64-slice Brilliance CT (Philips Healthcare, Amsterdam, NL), with a slice thickness of 1 mm.

One patient underwent 2 CT examinations. The first one was performed shortly after the onset of hypoxemia and was nearly negative (presence of a shaded circumscribed bibasal ground-glass opacity [GGO]). The second one, which was performed after 46 hours, was positive and was used for image analysis.

Six CT studies were only available printed on x-ray films, whereas the others were stored in the picture archiving and communication system.

Two observers (M.P., G.D.) independently assessed the presence and extension of the CT signs of pulmonary involvement according to the current accepted terminology.[19] In particular, the following findings were noted: consolidations, GGO, lobular consolidation and lobular GGO, nodules, bronchial wall thickening, septal thickening, and crazy paving. Lobular GGO and lobular consolidations are opacities with polygonal margins due to the involvement of a whole secondary lobule or of a portion of it.

The distribution of GGO was classified as peribronchial, random (patchy), or diffuse. The distribution of consolidations was classified as gravitational (dependent) or antigravitational (asymmetric or patchy).

TABLE 2. Signs and Laboratory Findings

Patient	Age, y	Sex	Fracture	Petechial Rash	Cerebral Involvement	Thrombocytopenia	Hyperbilirubinemia	Others
1	19	M	Tibioperoneal R	No	No	Yes	Yes	P, A
2	30	M	Tibioperoneal L	Yes	No	Yes	No	A, P, T
3	20	M	Femoral L	No	No	Yes	Yes	TP, ESR, A,
4	35	M	Leg amputation L, tibioperoneal R	Yes	Yes	Yes	No	P, T, A, ESR
5	28	M	Femoral L, tibioperoneal R	Yes	Yes	Yes	Yes	ESR
6	22	M	Femoral R	Yes	Yes	Yes	Yes	P, T
7	18	M	Humeral L, femoral L, tibioperoneal L	Yes	No	Yes	No	P, C
8	26	M	Femoral L	Yes	Yes	Yes	No	A, P
9	22	F	Femoral L	Yes	No	Yes	Yes	A, BAL$^+$
10	25	M	Femoral L, humeral L	Yes	No	Yes	Yes	P, T, A
11	33	F	Femoral R	No	No	Yes	No	A, P,T
12	23	M	Femoral R	No	Yes	Yes	Yes	P, T, A
13	19	M	Femoral L	Yes	Yes	Yes	Yes	P, A
14	19	M	Tibioperoneal R, humeral L	Yes	No	Yes	Yes	P, T, A
15	31	M	Femoral L	Yes	Yes	Yes	Yes	P, T, A
16	37	M	Tibioperoneal L, femoral L	No	No	Yes	Yes	P, A, T, TP
17	58	F	Radioulnar R, ribs R, pelvis, patellar	Yes	No	Yes	Yes	A, P
18	29	F	Femoral L, peroneal L	No	No	Yes	Yes	A, TP, T, BAL$^+$

Clinical signs and laboratory findings leading to the diagnosis of FES.

M indicates male; F, female; R, right; L, left; T, tachycardia; TP, tachypnea; P, pyrexia; A, anemia; C, hypercreatinemia; ESR, erythrocyte sedimentation rate; BAL$^+$, macrophages laden with lipid inclusions at bronchoalveolar lavage.

The nodules were classified according to their size, in micronodules (<3 mm in diameter) or nodules, and according to their density, as solid or ground glass.

After the evaluation of interobserver variability by means of the κ statistics, a final decision on the presence of the findings was reached by consensus.

To assess the predominance of the distribution of the lesions and for the correlation with clinical picture, we developed a CT scoring system that took into account the parenchymal extension of 3 findings (consolidations, GGOs, and nodules). The observers assessed the scores visually. The score was elaborated separately for each finding and separately for each pulmonary lobe as follows: 0 = no involvement, 1 = less than 30% of the parenchyma, 2 = less than 60%, and 3 = more than 60%. The sums of the scores of the various lobes gave the CT scores that were calculated for each single finding, as well as globally, for whole pulmonary involvement (we assigned a weighting of 0.5 for the middle lobe and the lingual).

Computed tomographic angiograms of the pulmonary arterial vessels were available for 4 patients. Three were performed with a Hi-speed multislice (GE Medical System), and one was performed with a 64-slice Brilliance CT (Philips Healthcare). They were reviewed for the presence of macroscopic fat emboli.

Statistical Analysis

Interobserver variability was measured using the κ statistic. The Mann-Whitney U test was used to assess the distribution of pulmonary involvement for each CT sign and the global score. Lobar distribution was compared between upper lobes or lower lobes, excluding the middle lobe and lingual. Lateral prevalence was compared as well.

The relationship between the CT findings and the severity of the clinical picture was assessed using Spearman correlation coefficient. As a clinical parameter reflecting the severity of the

respiratory involvement, the duration of the respiratory failure was chosen, expressed as the number of days of assisted ventilation (invasive and noninvasive) the patients required (Table 3). Correlations were considered significant at the 0.05 level.

Statistical analyses were performed using Internet-based, free calculators (http://www.graphpad.com; http://www.socscistatistics.com).

RESULTS

Clinically, 13 patients presented with a transient respiratory failure, whereas 5 developed ARDS (4 moderate, 1 severe). No patient had the fulminant form.

The prevalence of the various CT finding and the relative k values are listed in Table 4.

Bilateral consolidations were seen in 17 patients (94%) with dependent distribution in 13 (76%) of 17 and nondependent distribution in 4 (24%) of 17.

Seventeen patients (94%) showed GGO, and the distribution was random in 14 (82%) of 17, diffuse in 2 (12%) of 17, and peribronchial in 1 (5%) of 17 (Fig. 1).

Lobular GGOs were present in 11 patients (61%), and lobular consolidations were present in 11 patients (61%) (Fig. 2).

In total, 15 patients (83%) showed presence of nodules (Fig. 3), of which ground-glass nodules were apparent in 9 patients (50%); ground-glass micronodules were apparent in 8 patients (44%); solid nodules were apparent in 10 patients (55%); and solid micronodules were apparent in 13 patients (72%). The nodules and micronodules always showed a random distribution (centrilobular and subpleural distribution).

Smooth septal thickening was present in 9 patients (50%). Bronchial wall thickening was present in 12 patients (66%) (Fig. 4).

Areas of the crazy paving pattern were seen in 4 patients (22%) (Fig. 5). Crazy paving was extensive in only 1 patient and

TABLE 3. CT Scores and Clinical Parameters

Patient	Slice Thickness, mm	ARDS	Assisted Ventilation, d	CT Scores	Consolidations Scores	Nodules Score	GGO Scores
1	1.25	No	2	15.5	4	4	7.5
2	2	No	7	20	4	6	10
3	1.25	No	2	17	4	4.5	8.5
4	5	Yes (moderate)	12	20.5	8	4.5	8
5	2.5	No	8	17	8	4	5
6	5	No	7	3	3	0	0
7	5	No	NA	12	4	4	4
8	2.5	No	4	13	3	0	10
9	5	Yes (moderate)	NA	21.5	7	4.5	10
10	5	Yes (severe)	NA	19	8	5.5	5.5
11	1.25	No	1	8.5	1	0	7.5
12	7	No	7	15.5	2	6	7.5
13	8	No	3	13.5	0	3	10.5
14	8	Yes (moderate)	12	19	7	6	6
15	5	Yes (moderate)	15	21	8	6	7
16	5	No	4	19	4	8	7
17	1	No	3	17	4	6	7
18	10	No	3	17	2	7	8

For each patient, slice thickness, presence and severity of ARDS, the overall score and the score relative to the extension of nodular involvement, GGO, and consolidations and duration of assisted ventilation are reported.

NA indicates not available.

TABLE 4. Prevalence of Pulmonary CT Findings and the Relative *k* Values

Finding	No. of Patients	%	*k*
Consolidations	17	94	0.64
GGO	17	94	0.643
Lobular consolidations	11	61	0.76
Lobular GGOs	11	61	0.65
Nodules	15	83	
Solid nodules	10	55	0.67
Ground-glass nodules	9	50	0.67
Solid micronodules	13	72	0.72
Ground-glass micronodules	8	44	0.39
Smooth septal thickening	9	50	0.77
Crazy paving	4	22	0.57
Bronchial wall thickening	12	66	0.50
Pleural effusion	9	45	0.76

showed limited spatial extension in the others. Pleural effusion was present in 9 patients and was always limited and bilateral.

All the 5 patients who developed clinical ARDS showed presence of extensive consolidations and GGO. Of them, 4 showed extensive GGOs and dependent consolidations, with an anterior-posterior density gradient, whereas 1 patient showed patchy distribution of the consolidations. They all showed presence of an overlapping nodular pattern as well, although with variable extension.

In 4 patients, CT angiograms were available: from the revision of the contrast-enhanced scans, no evidence of macroscopic fat emboli was found in the pulmonary arteries.

The results of the Spearman correlation test are displayed in Table 5. The overall CT scores and the consolidation scores show a positive significant correlation with the duration of assisted ventilation.

The distribution of the global CT scores did not differ between the upper and lower lobes and right and left lung at a statistically significant level. Nodules and GGO were more prevalent in the upper lobes, whereas consolidations were more prevalent in the lower lobes, and both these differences had statistical significance.

The extent of the findings was extremely variable between the patients. The lung involvement by GGOs was, on average, the most extensive. Whereas in some patients nodular involvement was extensive, in others it was more limited, and in some it was absent.

DISCUSSION

The variability of the incidence of FES reported in the literature is due to the different diagnostic criteria adopted. The criteria from Gurd and Wilson[3] are the most widely adopted and show a lower incidence of FES than those from Lindeque et al.[5] To obtain a higher diagnostic confidence in our series, we chose to include only patients with a clinical picture fitting the criteria from Gurd and Wilson.

Still, a clear understanding of the pathophysiology of FES is lacking, but there is some agreement that the pathological process takes place in 2 phases and takes into account both the mechanical and biochemical hypotheses.[1,20] Immediately at the time of injury, the mechanical phase occurs, in which fat droplets
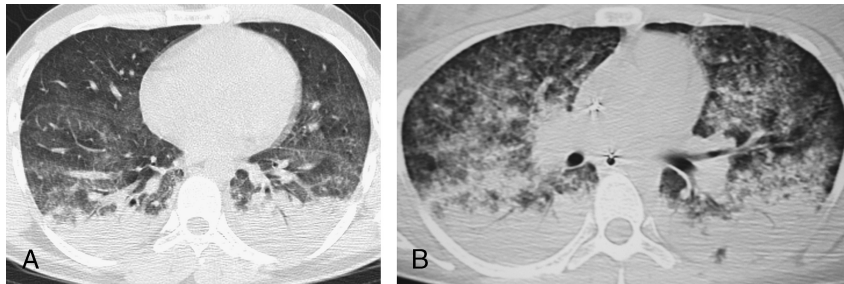
FIGURE 1. Fat embolism syndrome in 2 patients with a femoral fracture. A, 26-year-old man. Lung CT shows patchy, GGO, and bilateral, gravity-dependent consolidations. B, A 22-year-old woman. Fat embolism syndrome with ARDS. Lung CT shows the presence of an extensive gravitational density gradient (note the overlapping micronodular pattern with random distribution).
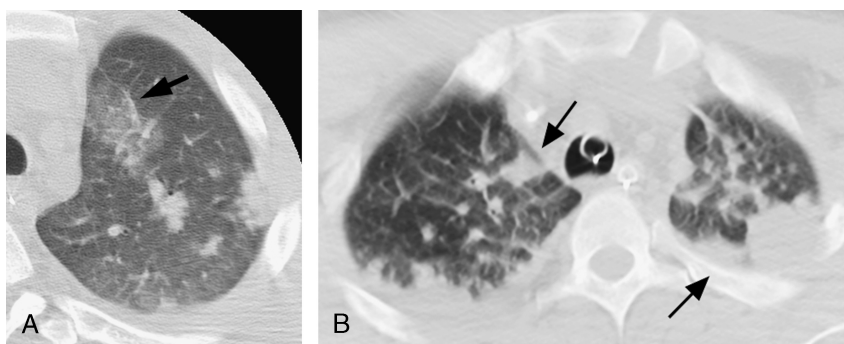
FIGURE 2. Lobular opacities in FES. A, Computed tomography shows lobular ground opacity (arrow) and scattered areas of lobular consolidations in the left upper lobe. B, Bilateral lobular consolidations in the upper lobe (arrows), showing polygonal shape.
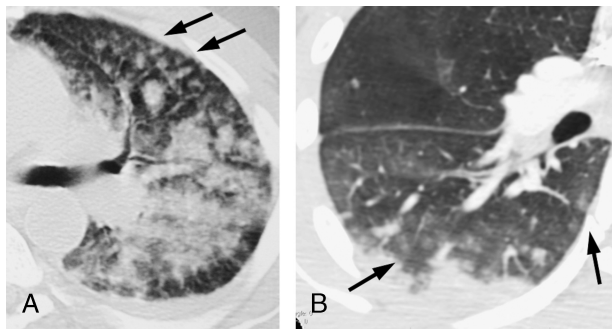
FIGURE 3. Nodular pattern in 2 different patients with a diagnosis of FES. In both patients, consolidations and bronchial wall thickening also coexisted. A, A 37-year-old man with a femoral fracture. Solid nodules (arrows) with random distribution (centrilobular and subpleural). B, A 19-year-old man with a tibial-fibular fracture, with ground-glass nodules and micronodules (arrows).

are released into venous blood, causing embolization and mechanical obstruction of the pulmonary and systemic capillary bed. How fat droplets arrive at systemic circulation is not clear, and the most accepted hypotheses are that this occurs through a patent foramen ovale or through the pulmonary capillary bed. After a latent phase, the biochemical phase occurs and is due to the toxic and biochemical effects of free fatty acids and of other, partly unknown, mediators. The pulmonary response is variable and characterized by events, such as permeability edema, vasculitis, or inflammation.[1,4,6,20]

To our knowledge, in the literature, there are only a few studies that have described the histopathology of FES in human patients. More frequently, the pathologic pattern described is that of a toxic vasculitis with alveolar hemorrhage, in which the presence of fat droplets in the alveolar capillaries and alveolar spaces is accompanied by concomitant interstitial and alveolar hemorrhage and edema.[7,21–25] While alveolar hemorrhage is a frequent histologic finding, the clinical presentation of FES as diffuse alveolar hemorrhage is rare, and this discrepancy may be due to the lack of the use of bronchoalveolar lavage.[25]

Permeability edema without evidence of hemorrhage and necrosis has also been reported,[7] as has the development of membrane hyaline,[7,21,24,26] which is the histologic hallmark of the acute phase of diffuse alveolar damage (DAD) and is the histologic correlate of ARDS.[27] The severe inflammatory response leading to ARDS/DAD after trauma can be triggered by several factors. Some of these factors are well known, such as transfusions or sepsis, whereas others are still unknown. The pathogenic role of FE in the development of ARDS has not been fully elucidated, but is a probable trigger of this condition, perhaps in conjunction with other mediators.[6]

We found that the lung CT findings somehow correlated with the histopathologic patterns. Two patients had a nearly completely negative CT scan immediately after the onset of hypoxemia, with a remarkable change to the positive at a subsequent CT scan after 45 hours in 1 case and at follow-up x-rays in the other (Fig. 6). Clinical-radiological dissociation is already known from conventional radiology[8–10] and is also reported at CT.[28] As such, radiologists should be aware of the possibility of a negative CT examination. Specifically, it can be assumed that, in presence of
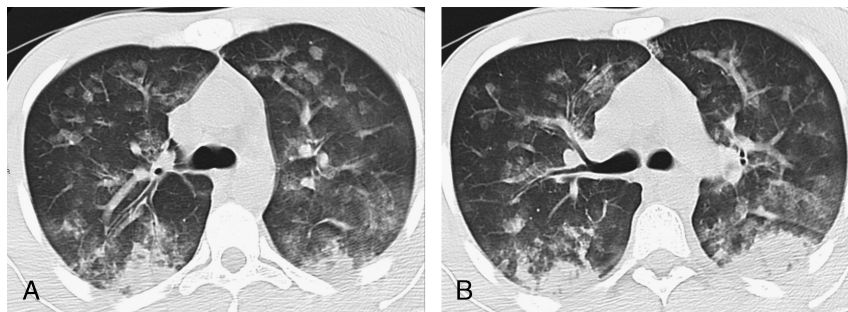
FIGURE 4. Fat embolism syndrome in a 20-year-old man with a femoral fracture. A and B, Diffuse lung involvement characterized by bilateral lobular GGOs, ground-glass nodules, GGOs, bilateral gravity-dependent consolidations, and bronchial wall thickening.
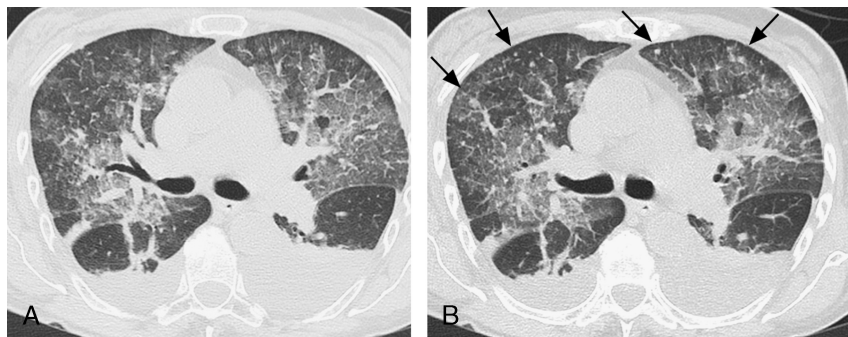
FIGURE 5. Fat embolism syndrome in a 58-year-old woman after fractures of the pelvis, patella, and ulna. A, High-resolution CT scan reveals extensive, bilateral crazy paving pattern, with perihilar distribution. B, Maximum intensity projection reconstruction at the same level. Presence of overlapping solid micronodules and nodules, which are better depicted with maximum intensity projection.

TABLE 5. Results of the Correlations Between the CT Findings and the Duration of Assisted Ventilation (Resolution)

Spearman ρ		Overall CT Score	Nodules Score	Ground Glass Score	Consolidations Score
Resolution	Correlation coefficient	0.572	0.250	−0.380	0.636
	P	**0.025**	0.368	0.161	**0.010**
	n	15	15	15	15

Bold font mean values are significant.

hypoxemia and CT negativity, the respiratory failure may mainly be due to the mechanical phase of FES or that the study was performed too quickly after the onset or that the biochemical and inflammatory response to FE was weak.

The random distribution of nodules is in line with the hematogenous genesis of the process. Like other authors,[11,12] we presume that the nodules may reflect foci of fat embolization into the pulmonary circulation, with initial capillary damage. It is likely that when the biochemical phase takes over, phenomena, such as permeability edema and hemorrhage, may spread around the secondary pulmonary lobule, resulting in the CT finding of focal areas of GGO or consolidation, with sublobular or lobular distribution. Interstitial edema also causes smooth septal thickening and the appearance of enlarged venules.

The patients with the ARDS were more likely to be those with the most severe inflammatory response and possibly with DAD. Of course, we can only speculate about the histopathologic features in our patients, because none of them underwent lung biopsy or autopsy.

The statistics showed that the severity of the clinical pictures correlated with the extent of consolidations, but not with that of nodules or GGOs. This is not surprising, because radiologically consolidations represent the complete replacement of alveolar air.

Regarding the presence of nodules in patients with FES, our results appear to agree with others' studies that are present in the literature. In 2000, Heyneman and Müller[11] reported a case of a patient with FES showing small nodular opacities, which were located in the centrilobular and subpleural regions. In the same year, Arakawa et al[12] published a study on 6 patients, showing nodular opacities ranging from 2 to 10 mm in diameter and gravity-dependent opacities, which were prevalent in the lower lobes, in all patients. In 2006, Gallardo et al[13] described the CT findings in 5 patients with FES, and nodules were seen in 4 patients with centrilobular and subpleural distribution. On the contrary, our results seem to contrast with another study that reported a nodular pattern in only 2 of 9 patients with mild FES.[14] In that study, high-resolution CT scans were performed, whereas in our series and in other studies, the patients had a volumetric CT examination.

This might explain the discrepancy between the findings because with conventional high-resolution CT the majority of the lung parenchyma is not covered, and the nodules might be lost.[29]

Clinically and radiologically, FES shares a differential diagnosis with several acute pulmonary diseases, such as traumatic lesions, ARDS, pneumonia, aspiration, hydrostatic pulmonary edema, and pulmonary embolism.

Pulmonary contusions typically appear as patchy airspace opacities or consolidations with ill-defined borders, subpleural sparing, and nonsegmental distribution. In general, they reach their maximum extension in 24–48 hours and are usually unilateral and asymmetric.[30,31] On the contrary, FES shows up after a latent period from the trauma, and the pulmonary alterations that result are usually bilateral and diffuse.

Adult respiratory distress syndrome shows 2 CT patterns. The typical pattern consists of extensive symmetric GGOs showing a classic anterior-posterior density gradient, with dependent consolidations, whereas the atypical pattern shows nondependent and asymmetric consolidations.[32–34] In our series, 3 patients showed a typical ARDS pattern, whereas one showed an atypical pattern. In all patients, there was an overlapping nodular involvement. Adult respiratory distress syndrome is often a multifactorial process, and because FE can be one of the triggers of this syndrome, perhaps it is not correct to refer to differential diagnosis between the 2 conditions.

Pneumonia may present and demonstrate several different patterns at CT.[35] Frequently, it has a lobular pattern, which is characterized by centrilobular nodules and tree-in-bud opacities. In our series, no patients presented with tree-in-bud opacities, and the nodules showed a random distribution. However, some viral pneumonia may also show nodules that are randomly distributed.[36]

Aspiration may show several patterns. A massive intake of gastric content may have dramatic consequences causing a severe chemical pneumonia (Mendelson syndrome); obstruction of the airways by foreign bodies does cause atelectasis with bronchial dilatation; more frequently, the aspirations present with lobar or segmental distribution, interesting posterior segments in the upper lobes, and superior segments in the lower lobes.[37]

FIGURE 6. A 30-year-old man with tibial-fibular fracture. Lung CT, which was performed 2 hours after the onset of the respiratory failure, reveals only circumscribed GGO in the left lower lobe (A); extensive bilateral GGOs, with nodules, septal thickening, micronodules, nodules, and dependent consolidations, were seen on a second CT scan, which was repeated 45 hours later (B, C).

Hydrostatic edema presents at CT with extensive smooth thickening of interlobular septa, pleural effusion, pulmonary venous enlargement, and GGOs. It tends to show upper lobar and peribronchial distribution.[38,39] In our series, the septal lines were recurrent, and GGOs were, in general, randomly distributed, although with a predominance in the upper lobes. The coexistence of the random nodules, in particular, if solid, may be helpful in the differential diagnosis.

Acute pulmonary embolism does not show specific pulmonary parenchymal alterations, apart from the peripheral wedge-shaped opacities.[40]

Although in the radiological literature there are some case reports of macroscopic fat emboli,[15–17] we did not encounter such findings in our series. Computed tomographic angiograms were available for only 4 patients. This could have contributed to the lack of detection of macroscopic emboli, which has to be considered, at present, as an exceptional occurrence. The detection of macroscopic fat emboli with CT angiography could become the object of future studies.

This study has several limitations. Because FES is a clinical diagnosis and biopsy is not routinely performed in patients with posttraumatic respiratory failure, we do not have pathological confirmations. Only 2 patients had some kind of pathological confirmation of disease, specifically, macrophages laden with lipid inclusions at bronchoalveolar lavage. The only clinical sign that allows for a nearly certain diagnosis of FES is the petechial rush, which was reported in 12 patients in our series. Although, to our knowledge, this is the largest series of CT studies in pulmonary FES available in the literature, the number of patients is, in itself, not large. This is a retrospective study. The CT techniques used in the studies were heterogeneous.

In conclusion, in our series of patients with a clinical diagnosis of FES, we found 3 CT patterns. First, the lung CT picture might be poor and nonspecific, virtually negative (but allowing to exclude presence of other conditions). Secondly, it may show a bilateral pulmonary involvement mainly characterized by patchy GGOs and dependent consolidations, variably associated with other overlapping signs, such as lobular opacities, random nodules, septal thickening, and bronchial wall thickening. Finally, patients who develop ARDS show extensive bilateral consolidations and GGOs, associated with nodular involvement.

ACKNOWLEDGMENTS

REFERENCES

1. Akhtar S. Fat embolism. *Anesthesiol Clin*. 2009;27:533–550.

2. Bolliger SA, Muehlematter K, Thali MJ, et al. Correlation of fat embolism severity and subcutaneous fatty tissue crushing and bone fractures. *Int J Legal Med*. 2011;125:453–458.

3. Gurd AR, Wilson RI. The fat embolism syndrome. *J Bone Joint Surg Br*. 1974;56B:408–416.

4. Mellor A, Soni N. Fat embolism. *Anaesthesia*. 2001;56:145–154.

5. Lindeque BG, Schoeman HS, Dommisse GF, et al. Fat embolism and the fat embolism syndrome. A double blind therapeutic study. *J Bone Joint Surg Br*. 1987;69:128–131.

6. Robinson CM. Current concepts of respiratory insufficiency syndromes after fracture. *J Bone Joint Surg*. 2001;Br 83:781–791.

7. Curtis AM, Knowles GD, Putman CE, et al. The three syndromes of fat embolism: pulmonary manifestations. *Yale J Biol Med*. 1979;52: 149–157.

8. Maruyama Y, Little JB. Roentgen manifestation of traumatic pulmonary fat embolism. *Radiology*. 1962;79:945–952.

9. Feldman F, Ellis K, Green WM. The fat embolism syndrome. *Radiology*. 1975;114:535–542.

10. Greenberg HB. Roentgenographic signs of posttraumatic fat embolism. *JAMA*. 1968;204:540–541.

11. Heyneman LE, Müller NL. Pulmonary nodules in early fat embolism syndrome: a case report. *J Thorac Imaging*. 2000;15:71–74.

12. Arakawa H, Kurihara Y, Nakajima Y. Pulmonary fat embolism syndrome: CT findings in six patients. *J Comput Assist Tomogr*. 2000;24:24–29.

13. Gallardo X, Castañer E, Mata JM, et al. Nodular pattern at lung computed tomography in fat embolism syndrome: a helpful finding. *J Comput Assist Tomogr*. 2006;30:254–257.

14. Malagari K, Economopoulos N, Stoupis C, et al. High resolution CT findings in mild pulmonary fat embolism. *Chest*. 2003;123:1196–1201.

15. Ravenel JG, Heyneman LE, McAdams HP. Computed tomography diagnosis of macroscopic pulmonary fat embolism. *J Thorac Imaging*. 2002;17:154–156.

16. Nucifora G, Hysko F, Vit A, et al. Pulmonary fat embolism: common and unusual computed tomography findings. *J Comput Assist Tomogr*. 2007; 31:806–807.

17. Yeo SH, Chang HW, Sohn SI, et al. Pulmonary and cerebral fat embolism syndrome after total knee replacement. *J Clin Med Res*. 2013;5: 239–242.

18. Definition Task Force ARDS, Ranieri VM, Rubenfeld GD, et al. Acute respiratory distress syndrome: the Berlin definition. *JAMA*. 2012;307: 2526–2533.

19. Hansell DM, Bankier AA, MacMahon H, et al. Fleischner Society: glossary of terms for thoracic imaging. *Radiology*. 2008;246:697–722.

20. Peltier LF. Fat embolism. A perspective. *Clin Orthop Relat Res*. 1998;232: 263–270.

21. Berrigan TJ Jr, Carsky EW, Heitzman ER. Fat embolism. Roentgenographic pathologic correlation in 3 cases. *Am J Roentgenol Radium Ther Nucl Med*. 1996;96:967–971.

22. Dines DE, Burgher LW, Okakaki H. The clinical and pathological correlation of fat embolism syndrome. *Mayo Clinic Proc*. 1975;50: 407–411.

23. Kao SJ, Yeh DY, Chen HI. Clinical and pathological features of fat embolism with acute respiratory distress syndrome. *Clin Sci (Lond)*. 2007; 113:279–285.

24. Choi JA, Oh YW, Kim HK, et al. Nontraumatic pulmonary fat embolism syndrome: radiologic and pathologic correlations. *J Thorac Imaging*. 2002; 17:167–169.

25. Froidure M, Baudouin N, Merati M, et al. Fat embolism with lung hemorrhage. *Rev Mal Respir*. 2001;18(6 pt 1):657–660.

26. Caper TH. Pulmonary hyaline membrane formation in the adult. *Am J Med*. 2001;31:701–710.

27. Castro CY. ARDS and diffuse alveolar damage: a pathologist's perspective. *Semin Thorac Cardiovasc Surg*. 2006;18:13–19.

28. Trisolini R, Cancellieri A, Giovannitti A, et al. Fat embolism may be responsible for hypoxemia in trauma patients with no radiological pulmonary abnormalities. *J Trauma*. 2010;68:E53–E54.

29. Primack SL, Müller NL, Mayo JR, et al. Pulmonary parenchymal abnormalities of vascular origin: high-resolution CT findings. *Radiographics*. 1994;14:739–746.

30. Kaewlai R, Avery LL, Asrani AV, et al. Multidetector CT of blunt thoracic trauma. *Radiographics*. 2008;28:1555–1570.

31. Mirka H, Ferda J, Baxa J. Multidetector computed tomography of chest trauma: indications, technique and interpretation. *Insights Imaging*. 2012;3: 433–449.

32. Goodman LR, Fumagalli R, Tagliabue P, et al. Adult respiratory distress syndrome due to pulmonary and extrapulmonary causes: CT, clinical, and functional correlations. *Radiology.* 1999;213:545–552.

33. Desai SR, Wells AU, Suntharalingam G, et al. Acute respiratory distress syndrome caused by pulmonary and extrapulmonary injury: a comparative CT study. *Radiology.* 2001;218:689–693.

34. Desai SR. Acute respiratory distress syndrome: imaging of the injured lung. *Clin Radiol.* 2002;57:8–17.

35. Herold CJ, Sailer JG. Community-acquired and nosocomial pneumonia. *Eur Radiol.* 2004;14(suppl 3):E2–E20.

36. Franquet T. Imaging of pulmonary viral pneumonia. *Radiology.* 2011; 260:18–39.

37. Kim M, Lee KY, Lee KW, et al. MDCT evaluation of foreign bodies and liquid aspiration pneumonia in adults. *Am J Roentgenol.* 2008;190: 907–915.

38. Komiya K, Ishii H, Murakami J, et al. Comparison of chest computed tomography features in the acute phase of cardiogenic pulmonary edema and acute respiratory distress syndrome on arrival at the emergency department. *J Thorac Imaging.* 2013;28:322–328.

39. Storto ML, Kee ST, Golden JA, et al. Hydrostatic pulmonary edema: high-resolution CT findings. *Am J Roentgenol.* 1995;165:817–820.

40. Shah AA, Davis SD, Gamsu G, et al. Parenchymal and pleural findings in patients with and without acute pulmonary embolism detected at spiral CT. *Radiology.* 1999;211:147–153.